Computer Simulation of Transport Driven Current in Tokamaks

W. J. Nunan and J. M. Dawson

Department of Physics, 405 Hilgard Avenue, University of California at Los Angeles, Los Angeles, California 90024-1547

(Received 24 November 1993)

We have investigated transport driven current in tokamaks via 2 + 1/2 dimensional, electromagnetic, particle-in-cell simulations. These have demonstrated a steady increase of toroidal current in centrally fueled plasmas. Neoclassical theory predicts that the bootstrap current vanishes at large aspect ratio, but we see equal or greater current growth in straight cylindrical plasmas. These results indicate that a centrally fueled and heated tokamak may sustain its toroidal current, even without the "seed current" which the neoclassical bootstrap theory requires.

Tokamak fusion plasmas will generate large self-driven current, and this will have a great impact on steady-state reactor designs. To gain a deeper understanding of such current drive mechanisms, we have performed fully electromagnetic (EM), particle-in-cell (PIC) computer simulations which demonstrate steadily rising toroidal current not only at typical aspect ratios of four, but also in straight cylinders (infinite aspect ratio). This transport driven current exceeds that predicted by the neoclassical bootstrap current theory [1–3], but follows from the conservation of the toroidal or z component of the particles' canonical momentum.

The "2 + 1/2 dimensional" PIC code computes (x, y, v_x, v_y, v_z) (from the Lorentz force) for all electrons and ions and calculates the fully self-consistent EM fields within rectangular, perfectly conducting boundaries. The z coordinate is ignorable due to the assumed symmetry and corresponds to the toroidal coordinate. The x coordinate corresponds to the major radius with a constant offset. Although there are no gradients in the $\hat{z}$ direction, the particles flow in that direction and give rise to a current density (J_z) which forms the self-consistently computed, time varying, poloidal field. The field solver geometry is Cartesian; however, in the "quasitoroidal" runs, we introduce an externally applied $B_z = B_{z0}x_0/(x + x_0)$. This field causes a ∇B drift of the particles, which is an important toroidal effect.

The plasma is initialized with a parabolic profile [$n_i = n_e = n_0(1 - r^2/a^2)$], a uniform temperature profile $(T_i = T_e = T_0)$, and a net toroidal current. The magnitude of the external, uniform, $\hat{y}$-directed, vertical field (B_v) is chosen so that the $J_z \times B_v$ force counterbalances the plasma's tendency to drift in the $\hat{x}$ direction due to ∇B_z. After a brief time at the beginning of the run, the plasma relaxes into equilibrium with $\vec{J} \times \vec{B} \approx \nabla p$ and $\nabla \cdot \vec{J} \approx 0$.

When particles reach a circular "limiter" near the edge of the grid, they are removed from the system, and their positions, velocities, etc., are saved for diagnostic purposes. The square, conducting walls deform the outer flux surfaces and constant potential surfaces, so that they are slightly noncircular, and, therefore, not exactly

parallel to the limiter. These deformations cause greater particle loss at the "corners," where the flux and potential surfaces cross the limiter, than at points where the limiter, conducting wall, potential surfaces, and flux surfaces are parallel.

New ion-electron pairs are injected into the plasma to sustain the density. These reinjected particles have a temperature of T_0, but, unlike the initial particles, have no net average drift velocity or current in the $\hat{z}$ direction. The spatial profile of this refueling may be a hollow annulus, to simulate edge fueling due to gas puffing or particle recycling from the walls, or may be centrally peaked, to approximate neutral beam or pellet fueling.

Although particles are always injected as net neutral pairs, the ions initially escape more rapidly than the electrons due to their larger orbits. This gives rise to a net charge density in the plasma and a radial electric field at the plasma's edge, as can be seen in Fig. 1. The code recomputes the fields every time step, but the magnitude of the radial E field at the edge is established very early in the run, and only the detailed shape of the internal potential contours continues to vary.

In these simulations, $\vec{E} \times \vec{B}$ drifts are the dominant transport mechanism. These drifts are parallel to contours of constant electrostatic potential which typically are as shown in Fig. 1. The particles execute trajectories which,
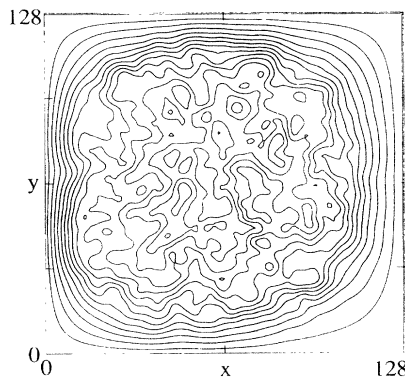
FIG. 1. Contours of constant electrostatic potential.

in the quasitoroidal runs, can resemble arcs of banana orbits, but the fluctuating $\vec{E} \times \vec{B}$ drifts prevent such orbits from persisting for as long as a bounce time.

Figure 2 shows the normalized current $(\mu_0 I_z/aB_z)$ vs normalized time $(\omega_{ci}t)$ for three different simulations: an edge-fueled quasitorus, a centrally fueled quasitorus (both with aspect ratios of four), and a centrally fueled straight cylinder. All runs have $2\mu_0 p_{max}/B_z^2 = 4\%$ and $2\mu_0 p_{max}/B_\theta^2(a) = 4$ at $t = 0$. Initially the quasitoroidal plasmas are not exactly in equilibrium and, therefore, lose particles and current faster than the straight cylinder. Later, the centrally fueled runs with and without ∇B_z have similar rates of particle loss and current rise; therefore, banana orbits are not crucial to the results of these simulations.

What is critical is the position of the particle fueling. The edge-fueled case shows some current rise, but at a much lower rate than the centrally fueled plasmas, despite the fact that the particle loss and fueling rates are an order of magnitude greater. The total number of particles removed at the limiter during the run divided by the total number of particles in the plasma is 12.5% for the centrally fueled straight cylinder, 20.8% for the centrally fueled quasitorus, and 326% for the edge-fueled quasitorus.

In this PIC code, all quantities are independent of z; therefore, each particle conserves the $\hat{z}$ component of its canonical momentum:

$$p_{jz} = m_j v_{jz} + e_j A_z(\vec{r}_j, t). \qquad (1)$$

Here the subscript j denotes the jth particle, and the initial value of the canonical momentum is established at the time when the jth particle is injected. A collision subroutine has been added which models Coulomb scattering and breaks this p_{jz} conservation in a controlled way. When the collisions are "turned on," even with ν_{ei}/ω_{pe} set to a value orders of magnitude greater than is typical of tokamaks, the current drive still occurs.

This code requires the use of small time steps (on the order of the electron cyclotron period) and, therefore, large amounts of computer time. We, therefore, ran the simulations with greatly increased electron mass [= (ion mass)/9] and rather small system sizes (diameter of 85 ion Larmor radii). Because it is not practical to run
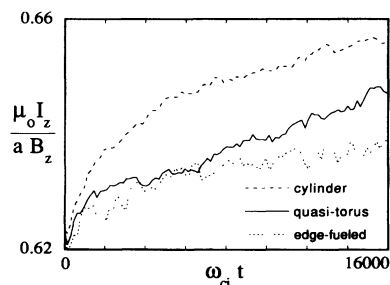
such a simulation for times on the order of the plasma's resistive time scale, we primarily focus on the results of collisionless simulations in this paper.

Given the complicated shape of the $\vec{E} \times \vec{B}$ drifts, it may not be obvious that p_{jz} is actually conserved, but Figs. 3 and 4 show that it is. The "birth" velocity distribution f_b is the distribution of the initial velocities of those particles which have been lost to the limiter. The function f_c is the calculated distribution function of $v_{zfinal} + \Delta A_z e_j/m_j$, which would be identical to f_b if the particles' canonical momenta were conserved. For the ions, f_b and f_c are barely distinguishable. The electrons' higher velocities make them slightly collisional (due to discrete particle and numerical effects), and so their f_c curve is slightly shifted from f_b.

The shape of f_b indicates that "costreaming" particles, which have $e_j v_{jz}$ of the same sign as J_{z0}, are better confined than "counterstreaming" particles, whose $e_j v_{jz}$ have the opposite sign of J_{z0}. As stated above, reinjected particles are given random velocities with a Maxwellian distribution and zero average; however, when the plasma is initially loaded, the particles are given an average drift such that the plasma has current in the $+\hat{z}$ direction. The $\hat{z}$ electron drift velocity is negative; the $\hat{z}$ ion drift velocity is positive and smaller in magnitude by a factor of m_e/m_i. Thus, the plasma initially has current but no net $\hat{z}$ kinematic momentum.

If the particles which are lost at the limiter were randomly selected from the initial particle distributions, then f_b and f_c should have Maxwellian shapes and small shifts in the positive direction for ions and in the negative direction for electrons. Figures 3 and 4 clearly show that the shifts are of greater magnitudes and in opposite directions. The counterstreaming particles reach the limiter in much greater numbers than the better confined costreaming particles. Particles opposing the net current are lost from the center of the plasma more readily than those enhancing it, and this drives net current even at the magnetic axis, in contrast to the neoclassical bootstrap theory.

These simulation results of current drive and preferential loss of counterstreaming particles emerge from a very

FIG. 2. Current versus time.
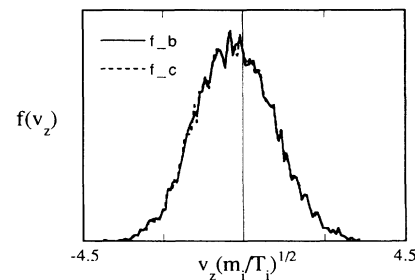
FIG. 3. Distribution of birth velocities of ions lost to the limiter.
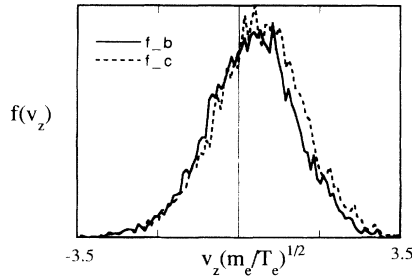
FIG. 4. Distribution of birth velocities of electrons lost to the limiter.

long computation involving hundreds of thousands of dynamical variables, and yet the main results can be understood in terms of a surprisingly simple conceptual model based on conservation of energy and p_{jz} and an assumed current profile. With these assumptions one can determine bounds on the radial motion of the particles without knowing the details of the potential profile of flow vortices.

A uniform current density J_{z0} over a cylinder of radius a generates a vector potential $A_z = \mu_0 J_{z0}(a^2 - r^2)/4$. If p_{jz} is conserved, then each particle's v_{jz} varies with radial position:

$$\Delta v_{jz} = e_j \mu_0 J_{z0} \Delta(r_j^2)/4m_j . \qquad (2)$$

If a particle moves outward $[\Delta(r_j^2) > 0]$, then its incremental contribution to the plasma current $(e_j \Delta v_{jz})$ has the same sign as J_{z0}; therefore, radial transport of both ions and electrons enhances the existing current.

Since it is energetically impossible for $|v_{jz}|$ to increase arbitrarily for all particles, there is a significant constraint on the particle motion. We denote the jth particle's initial velocity as $\vec{v}_{j0}$, and $v_{j0} = |\vec{v}_{j0}|$. If the particle conserves kinetic energy (as it would tend to while $\vec{E} \times \vec{B}$ is drifting along a surface of constant potential) then $-v_{j0} \leq v_{jz} \leq v_{j0}$. Equation (2) relates this range of accessible velocities to the corresponding range of accessible radial positions: $r_{j\min} \leq r_j \leq r_{j\max}$, where

$$r_{j\min}^2 = r_{j0}^2 - \delta_j^2 v_{jz0}/v_{j0} - |\delta_j^2|, \qquad (3)$$

$$r_{j\max}^2 = r_{j0}^2 - \delta_j^2 v_{jz0}/v_{j0} + |\delta_j^2|, \qquad (4)$$

$$\delta_j^2 = 4m_j v_{j0}/e_j \mu_0 J_{z0} . \qquad (5)$$

If Eq. (4) gives $r_{j\max}^2 > a^2$, then the particle hits the limiter, is neutralized, and contributes no current. If Eq. (3) gives $r_{j\min}^2 < 0$, then, of course, the particle's $r_{j\min} = 0$.

Equations (3)—(5) show that particles in different regions of velocity space diffuse (in position space) at very different rates. First, Eq. (5) shows that a particle's collisionless step length (and, therefore, its diffusion coefficient, in the collisional case) increases with mass and energy. Second, Eq. (4) shows that a particle with

$\delta_j^2 > 0$ and $\vec{v}_{j0}$ parallel to $\hat{z}$ (or $v_{jz0} = v_{j0}$) cannot move outward from its initial position, and likewise for a particle with $\delta_j^2 < 0$ and $\vec{v}_{j0}$ antiparallel to $\hat{z}$ (or $v_{jz0} = -v_{j0}$). Both such particles carry current in the same direction as J_{z0}.

If the direction of the particles' initial velocities are reversed in these examples, then the particles have the largest possible $r_{j\max}$ for that initial position and energy. These are the limiting cases of a general trend that costreaming particles are better confined than counterstreaming particles, or that current filaments attract if they carry currents in the same direction and repel if they carry opposing currents. This applies to banana orbiting particles, but also to particles in a straight cylinder, in which banana orbits do not exist.

The differential loss rate of counterstreaming and costreaming particles constitutes an additional current drive mechanism. Particles opposing the net current are lost from the center of the plasma more rapidly than those enhancing it, resulting in net current drive, which we compute as follows: We assume that each particle is equally likely to be at any radial position within its allowed range of motion. The jth particle contributes a current density of

$$J_{jz} = \frac{e_j v_{jz}}{\pi(r_{j\max}^2 - r_{j\min}^2)\lambda} \qquad (6)$$

for $r_{j\min} \leq r \leq r_{j\max}$, and $J_{jz} = 0$ for r outside this range. The number of identical particles per unit length in the $\hat{z}$ direction is λ^{-1}.

Equation (2) combined with the particle's initial conditions specify v_{jz} as a function of r_j. Here we consider only the current generated at $r = 0$ by particles born at $r = 0$. In this case, $r_{j\min} = 0$, and Eq. (4) specifies $r_{j\max}$.

Averaging J_{jz} over a Maxwellian initial velocity distribution for species s yields the incremental current density for that species at $r = 0$ due to fueling:

$$\Delta J_{sz} \approx 0.2\mu_0 J_{z0} e_s^2 m_s^{-1} S_s \Delta t, \qquad (7)$$

where $S_s \Delta t$ denotes the number of particles per unit length injected at $r = 0$ during a time interval Δt. This mechanism acting on both electrons and ions produces an effective electric field:

$$E_{\text{eff}} \approx 0.2\mu_0^2 e^2 (Z^2/m_i + Z/m_e)a^2 J_{z0} S_i, \qquad (8)$$

where $e_i = eZ$. Extending this calculation to $r > 0$ and including more realistic fueling profiles is quite difficult analytically, but can readily be done numerically. The above argument does show that fueling on-axis drives current on-axis.

The analytical calculation is complicated by the fact that Eq. (3) becomes invalid if it gives $r_{j\min}^2 < 0$, in which case the particle's $r_{j\min}$ actually equals zero. A similar problem arises near the edge of the plasma, where Eq. (4) can give $r_{j\max}^2 > a^2$, in which case the particle leaves the system. For regions of the plasma $0 \ll r \ll a$ one

can make a simple estimate of the particle transport and current drive.

The random walk step length of the jth particle (between collisions) is $\Delta r_j = (r_{j\,\text{max}} - r_{j\,\text{min}})/2$. If $r_{j\,\text{min}} \gg \Delta r_j$ then Eqs. (3) and (4) give

$$\Delta r_j \approx |\delta_j^2|/2r_{j\,\text{min}} . \tag{9}$$

Averaging δ_j^2 over a Maxwellian velocity distribution for all particles of species s yields

$$\delta_s^2 = 8\sqrt{(2/\pi)m_s T_s}/e_s \mu_0 J_{z0} . \tag{10}$$

Combining the average step length with the decorrelation time of p_{jz} yields the diffusion coefficient for the particles. The fact that experiments do not exhibit anomalously large parallel resistivity suggests that turbulence effects are less important than collisions in defining the decorrelation time of the canonical momentum of the particles. Assuming that the decorrelation time for electron canonical momentum is the electron-ion collision time ($\tau_{ei} = m_e/e^2 n_e \eta$, where η is the classical resistivity) yields a diffusion coefficient for electrons:

$$D_e = \frac{\delta_e^4}{4r^2 \tau_{ei}} = \frac{4\eta}{\pi \mu_0} \left(\frac{2\mu_0 n_e T_e}{B_\theta^2} \right), \tag{11}$$

where $B_\theta = \mu_0 J_{z0} r/2$.

As in neoclassical theory, one may assume that the electron diffusion coefficient determines the ambipolar transport. For comparison, the banana diffusion coefficient [1] is $D_b = D_e \sqrt{2r/R_0}$. One can estimate the current driven by this particle transport using Ohm's law: $\eta J_z = E_z + v_r B_\theta$ and Fick's law $n v_r = -D \partial n/\partial r$:

$$J_z = \frac{E_z}{\eta} - \frac{8T_e}{\pi B_\theta} \frac{\partial n_e}{\partial r} . \tag{12}$$

Equation (12) resembles the neoclassical bootstrap current; however, Eqs. (11) and (12) and the neoclassical theory are not valid near the magnetic axis, where $D_b \to \infty$. Because the standard theory is not valid at the magnetic axis, any predictions about current drive (or an absence thereof) near the magnetic axis cannot be made using that theory; however, our simulation does treat the region near the axis correctly.

In summary, the neoclassical bootstrap current theory [2,3] asserts that a 100% bootstrapped tokamak is not achievable, but this prediction is inconsistent with both experimental data [4,5] and our simulations. Externally driven seed current appears to be unnecessary because of additional current drive at $r = 0$ due to the preferential loss of particles carrying current counter to the net plasma current.

[1] A. A. Galeev and R. Z. Sagdeev, Sov. Phys. JETP **26**, 233 (1968).

[2] R. J. Bickerton, J. W. Connor, and J. B. Taylor, Nature Phys. Sci. **229**, 110 (1971).

[3] B. B. Kadomtsev and V. D. Shafranov, in *Fourth International Conference on Plasma Physics and Controlled Nuclear Fusion Research, Madison, WI, 1971*, Vol. 2, p. 479 [Nucl. Fusion (Supplement), p. 209 (1972)].

[4] R. J. Taylor *et al.*, Bull. Am. Phys. Soc. **32**, 1747 (1987).

[5] C. B. Forest, Y. S. Hwang, M. Ono, and D. S. Darrow, Phys. Rev. Lett. **68**, 3559 (1992).